

Protein Interactions Studied by SAXS: Effect of Ionic Strength and Protein Concentration for BSA in Aqueous Solutions

Fajun Zhang,[†] Maximilian W. A. Skoda,^{†,‡} Robert M. J. Jacobs,[§] Richard A. Martin,[#] Christopher M. Martin,[‡] and Frank Schreiber^{*,†}

Institut für Angewandte Physik, Universität Tübingen, Auf der Morgenstelle 10, 72076 Tübingen, Germany, Physical and Theoretical Chemistry Laboratory, University of Oxford, South Parks Road, Oxford, OX1 3QZ, United Kingdom, Chemistry Research Laboratory, University of Oxford, 12 Mansfield Road, Oxford, OX1 3TA, United Kingdom, Department of Physics, University of Bath, Bath, BA2 7AY, United Kingdom, and SRS, Daresbury, Warrington, Cheshire, WA4 4AD, United Kingdom

Received: August 3, 2006; In Final Form: October 27, 2006

We have studied a series of samples of bovine serum albumin (BSA) solutions with protein concentration, c , ranging from 2 to 500 mg/mL and ionic strength, I , from 0 to 2 M by small-angle X-ray scattering (SAXS). The scattering intensity distribution was compared to simulations using an oblate ellipsoid form factor with radii of $17 \times 42 \times 42 \text{ \AA}$, combined with either a screened Coulomb, repulsive structure factor, $S_{SC}(q)$, or an attractive square-well structure factor, $S_{SW}(q)$. At $\text{pH} = 7$, BSA is negatively charged. At low ionic strength, $I < 0.3 \text{ M}$, the total interaction exhibits a decrease of the repulsive interaction when compared to the salt-free solution, as the net surface charge is screened, and the data can be fitted by assuming an ellipsoid form factor and screened Coulomb interaction. At moderate ionic strength (0.3–0.5 M), the interaction is rather weak, and a hard-sphere structure factor has been used to simulate the data with a higher volume fraction. Upon further increase of the ionic strength ($I \geq 1.0 \text{ M}$), the overall interaction potential was dominated by an additional attractive potential, and the data could be successfully fitted by an ellipsoid form factor and a square-well potential model. The fit parameters, well depth and well width, indicate that the attractive potential caused by a high salt concentration is weak and long-ranged. Although the long-range, attractive potential dominated the protein interaction, no gelation or precipitation was observed in any of the samples. This is explained by the increase of a short-range, repulsive interaction between protein molecules by forming a hydration layer with increasing salt concentration. The competition between long-range, attractive and short-range, repulsive interactions accounted for the stability of concentrated BSA solution at high ionic strength.

1. Introduction

Interactions between protein macromolecules in solution are a key factor in determining the phase behavior of biological systems. Also, the phase behavior determines whether one can get good quality protein crystals for X-ray diffraction, which is critical in obtaining the protein's three-dimensional structure and in elucidating its biochemical role.^{1–3} George and Wilson⁴ proposed a relation between protein crystallization behavior and the osmotic second virial coefficient, A_2 , which represents the interaction potential between a pair of macromolecules in solution. A positive value of A_2 implies a repulsive interaction, and a negative value indicates an attractive interaction. On the basis of measurements of a variety of proteins, they found that protein crystallization occurs only when A_2 lies within a narrow window. These studies provide a way to understand the mechanism of protein crystallization and a guide for optimization of conditions for protein crystallization.^{5–10} On the other hand, the protein interaction and aggregation processes are also very important in understanding many physiological problems,

for example, diseases such as Alzheimer or Kreutzfeld–Jacob and Parkinson, which are caused by protein or peptide association phenomena, and the short-range order of crystallin proteins accounts for the eye lens transparency.^{3,11} In vivo, the biochemical function of proteins cannot perform without the cooperation of the ions around them. Therefore, studies on the effect of ionic strength and the nature of ions on the protein interaction have attracted much attention in biophysics.^{5,6,12–15} Studies show that the interaction strongly depends on the nature of the salt used at a fixed ionic strength, which is known as the Hofmeister effect.^{5,6,13}

Protein solutions can be modeled as a charged, colloidal system, and their phase behavior under low ionic strength can be described by the Derjaguin–Landau–Verwey–Overbeek (DLVO) theory.¹⁶ The DLVO theory describes the interaction between charged colloids as a combined hard-sphere interaction, electrostatic repulsive interaction, and a van der Waals attractive interaction. Under low ionic strength, the DLVO theory describes the phase behavior of a protein solution satisfactorily.^{5,6,17} However, many studies indicate that the DLVO theory cannot fully explain the rich phase behavior of protein solutions.^{3,5,18–21} In some cases, a temperature-induced liquid–liquid phase separation has been observed in protein solutions.^{22,23} Theoretical and experimental studies indicate that a short-range attractive interaction is present and dominates the liquid–liquid phase separation and equilibrium cluster

* To whom correspondence should be addressed. E-mail: frank.schreiber@uni-tuebingen.de. Tel: ++49-7071-29-78663. Fax: ++49-7071-29-5110.

[†] Universität Tübingen.

[‡] Physical and Theoretical Chemistry Laboratory, University of Oxford.

[§] Chemistry Research Laboratory, University of Oxford.

[#] University of Bath.

[‡] SRS.

formation.^{5,6,12,13,24–28} Although the van der Waals attractive potential is able to account for the liquid–liquid phase separation of a protein solution without adding salt, other nonspecific interactions, such as hydration forces or hydrophobic interactions, may also be involved.^{5,6,27} For example, Petsev and Vekilov studied interactions of the protein apoferritin in aqueous solutions, and they found that the second osmotic virial coefficient exhibits a minimum when plotted as a function of salt concentration. They argue that the repulsive interaction at high salt concentration comes from a hydration effect.²⁹ In another example, Chen and co-workers^{12,13,30} studied lysozyme and cytochrome *c* under high salt concentration, and they found an increase of $I(0)$ and even a new peak at very low momentum transfer in small-angle neutron scattering (SANS). These results were also attributed to a short-range attractive interaction. Whether the increase of the forward intensity is induced by a weak, long-range attraction is still a matter of debate,^{30,31} and the nature of the attractive interaction potential rising from these studies is still not fully understood.

In this work, by using SAXS on BSA as a model system, we have systematically studied the effect of ionic strength on the protein–protein interaction using a large range of salt and protein concentrations. BSA is a globular protein, which is readily soluble in water and stable over a wide range of salt and protein concentrations. For BSA, no liquid–liquid phase separation behavior was reported, and under low ionic strength, the protein interaction is dominated by electrostatic repulsion. An attractive interaction was observed only at high ionic strength, $I \geq 1.0$ M. Therefore, we can distinguish this attractive potential induced by high salt concentration from other sources, such as van der Waals interactions.

2. Experimental Section

2.1. Materials. Bovine serum albumin (BSA) (product no. A7638) was purchased from Sigma-Aldrich. It is a lyophilized powder with a molar molecular weight of ~ 66 kDa and was used as received. A batch of solutions with 12 protein concentrations ranging from 2 to 500 mg/mL and 8 salt (NaCl) concentrations ranging from 0 to 2.0 M were prepared. Solutions with protein concentrations less than 100 mg/mL were prepared by diluting a stock solution, while the high protein concentration solutions, > 100 mg/mL, were prepared by directly dissolving the corresponding amount of protein powder in the solvent. Protein concentrations were determined by UV absorption based on absorption at wavelengths of 410 and 280 nm. The extinction coefficient of BSA at 280 nm is 39020/M/cm, or 0.5912/(mg/mL)/cm, calculated from the amino acid sequence.³² In order to avoid the affect of other ions, no buffer was used, and hence, the pH of all the solutions was ~ 7.0 .

2.2. Method. Small-angle X-ray scattering measurements were carried out on beamline 6.2 of the Synchrotron Radiation Source (SRS) at Daresbury Laboratory, Warrington, UK.³³ The beam energy was 15.0 keV, corresponding to a wavelength of 0.827 Å. The scattered intensity was registered with a 200-mm-radius quadrant detector located 3.3 m from the sample. The accessible q range was thus from 0.013 to 0.45 Å⁻¹. The detector response was calibrated using the scattering from water. The angular scale was calibrated using the scattering peaks of silver behenate.

Protein solutions were filled into a sample cell with two mica windows (25 μm thick) separated by a 1.0 mm Teflon spacer. In order to calculate the absolute intensity, the empty cell and salt solutions were also measured. All measurements were carried out at room temperature. The resulting data were

(electronically) converted to a 1D profile by integrating around an arc. The raw data were corrected for transmission, fluctuation of primary beam intensity, exposure time, and the geometry of the detector. The intensity was calibrated by the cross section of water by eq 1.³⁴ The final corrected data used for model fitting were

$$I(q) = \frac{d\sum(q)}{d\Omega_{\text{sample}}} = \frac{I(q)_{\text{sample}}}{I(0)_{\text{water}}} \times \frac{d\sum}{d\Omega_{\text{water}}} \quad (1)$$

where $I(q)_{\text{sample}}$ is the scattering intensity of the sample solution after correction, and $I(0)_{\text{water}}$ is the scattering intensity of water extrapolated to the origin; $d\sum/d\Omega_{\text{water}} = 0.01632 \text{ cm}^{-1}$ is the constant scattering intensity of water at 293 K. Note that the solvent scattering has been removed from all experimental data sets (Figures 1, 2, 4, and 5). The asymptotic behavior for large q values is then mostly determined by background scattering. When the curves are normalized to the protein concentration, the behavior is identical for all curves.

We note that, despite our efforts of calibrating the absolute intensity, the final cross section is lower by a factor of about two than that expected. We attribute this partially to the overestimation of transmission. However, this does not affect any of the conclusions regarding the interactions.

3. Data Analysis

Small-angle X-ray scattering is a very efficient technique to study the particle interaction in solution. The total scattering intensity, $I(q)$, for a monodisperse spherical system at a scattering angle of 2θ as a function of the scattering vector, $q = 4\pi\sin\theta/\lambda$, can be expressed by³⁵

$$I(q) = N_p(\Delta\rho)^2 V_p^2 P(q)S(q) \quad (2a)$$

where N_p is the number of protein molecules per unit volume in the solution, V_p is the volume of a single protein, and $\Delta\rho = (\rho_p - \rho_s)$ is the difference between the electron density of protein molecules and that of the solvent and is usually called the scattering contrast. $P(q)$ is the form factor of a given protein, that is, the scattering from a single protein molecule after orientational averaging. $S(q)$ is the structure factor, which contains information about the protein interactions.

For a polydisperse or nonspherical system, in an average structure factor approximation, eq 2a becomes

$$I(q) = N_p(\Delta\rho)^2 V_p^2 P(q)\bar{S}(q) \quad (2b)$$

$\bar{S}(q)$ is the effective structure factor and is calculated using a monodisperse structure factor at an effective sphere diameter. In our case, the protein solution is a monodisperse but nonspherical (ellipsoidal) system. The effective sphere diameter is calculated by equating the second virial coefficient, A_2 , of the ellipsoid to a sphere having the same A_2 .³⁶ This effective sphere diameter is then used to calculate the effective structure factor $\bar{S}(q)$.^{36,37}

In an ideal solution, where the protein molecules are well-separated from each other (i.e., there is no position or orientation correlation between them) $\bar{S}(q) = 1$, and the total scattering only has contributions from the form factor, $P(q)$. With increasing protein concentration, the interference effect between proteins cannot be neglected, and the structure factor becomes important in the total scattering intensity. $\bar{S}(q)$, in the low q range, strongly depends on the interaction potential between protein molecules. The structure factor at the origin, $\bar{S}(q = 0)$,

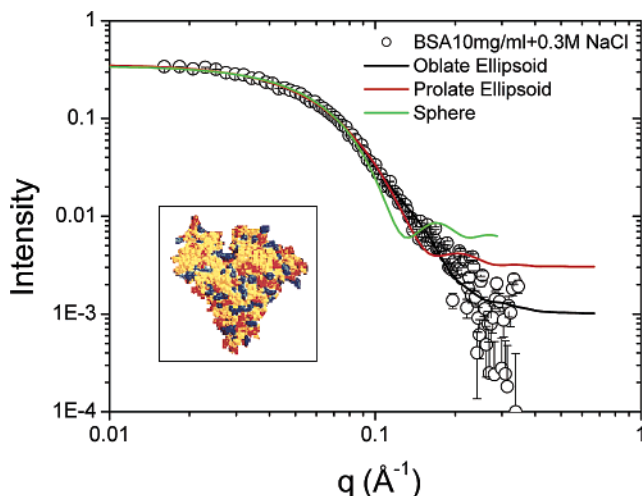


Figure 1. Scattered intensity and simulation by three form factors for a protein solution of 10 mg/mL with 0.3 M NaCl. It was shown that an oblate ellipsoid shape with $a = 17 \text{ \AA}$ and $b = 42 \text{ \AA}$ provided the best fit. Note that the calculated curves become constant for high q values since our model calculation includes a constant experimental background. The inset is the front view of the space-filling model of serum albumin with basic residues colored in blue, acidic residues in red, and neutral ones in yellow.

is equal to the normalized osmotic compressibility. With repulsive interactions, the protein molecules are uniformly distributed and $\bar{S}(0)$ is lower than unity, while with attractive interactions, fluctuations dominate the particle distribution and $\bar{S}(0)$ is larger than unity.^{5,6,27} Therefore, a detailed analysis of the $\bar{S}(q)$ can provide information on the nature of the interaction potentials.

The data analysis was done with the software package, IGOR Pro, using macros developed by the NIST center for neutron scattering research.³⁷ The neutron contrast term was replaced by an electron density difference term in the data-fitting procedure.

3.1. Protein Shape and Form Factor. The shape of BSA in solution was suggested to be a prolate ellipsoid with dimensions of $140 \times 40 \text{ \AA}$ with three domains aligned along the long axis. Therefore, early studies used a prolate ellipsoid form factor with radii of $a \times b \times b = 70 \times 20 \times 20 \text{ \AA}$.^{38,39} However, further studies indicated a heart-shaped structure, in agreement with X-ray crystallographic data.^{40,41} Recently, Ferrer et al.⁴² proposed an equilateral, triangular prismatic shell with a side length of 84 \AA and a thickness of 31.5 \AA . In this work, a general ellipsoid form factor (eq 3) was used to fit the data, and both the prolate and the oblate form factors were employed. We found that scattering data from a dilute protein solution can be successfully fitted by an oblate form factor with radii of $a \times b \times b = 17 \times 42 \times 42 \text{ \AA}$ (Figure 1), in good agreement with the model proposed by Ferrer et al.⁴²

$$P(q) \equiv \langle |F(q)|^2 \rangle = \int_0^1 dx \left| \frac{3(\sin u - u \cos u)}{u^3} \right|^2 \quad (3)$$

$$u = qb[(a/b)^2 x^2 + (1-x)^2]^{1/2}$$

3.2. Structure Factor. Protein-Protein Interaction Potential in Solution: According to Curtis,¹⁴ the interaction potential $U(r)$ for a pair of protein molecules in a salt solution with a center-to-center distance, r , can be expressed by the sum of the following spherically symmetric potentials:

$$U(r) = U_{\text{HS}}(r) + U_{\text{SC}}(r) + U_{\text{V}}(r) + U_{\text{OS}}(r) + U_{\text{A}}(r) \quad (4)$$

Here, $U_{\text{HS}}(r)$ is the hard-sphere potential related to the excluded-volume effect, $U_{\text{SC}}(r)$ is the screened Coulomb potential, $U_{\text{V}}(r)$ is the van der Waals attractive potential, $U_{\text{OS}}(r)$ is the depletion potential caused by the excluded-volume effect of the salt ions, and $U_{\text{A}}(r)$ is a potential employed to account for self-association of proteins. A general structure factor should consider all of the potentials described above. However, studies on the total interaction potential of proteins in salt solution indicate that, depending on the salt concentration, the interaction is dominated by only one or two of these potentials at any particular salt concentration. Therefore, the total potential can be simplified.

Screened Coulomb Structure Factor, $S_{\text{SC}}(q)$: At lower ionic strength, $I < 0.3 \text{ M}$, a structural model developed by Hayter and Penfold^{43,44} based on an interaction potential between charged, colloidal particles consisting of a hard sphere plus a screened Coulomb potential was used.

$$U_{\text{SC}}(r) = \begin{cases} \frac{z^2 e^2}{\epsilon(1 + \kappa_{\text{D}} R)^2} \frac{\exp[-\kappa_{\text{D}}(r - 2R)]}{r} & \text{for } r > 2R \\ \infty & \text{for } r \leq 2R \end{cases} \quad (5)$$

The charge of the protein, z , is assumed to be uniformly distributed on the surface, e is the electronic charge, and ϵ is the dielectric constant of the solvent. $R = 33.4 \text{ \AA}$ is the effective sphere radius of an oblate ellipsoid with $a \times b \times b = 17 \times 42 \times 42 \text{ \AA}$.³⁶ κ_{D} is the inverse of the Debye screening length and is determined by the ionic strength, I , of the solution.

$$\kappa_{\text{D}}^{-1} = \left(\frac{10^3 \epsilon k_{\text{B}} T}{8\pi e^2 N_{\text{A}}} \right)^{1/2} \quad (6)$$

The structure factor, $S(q)$, is the Fourier transformation of the spherically averaged pair correlation function, $g(r)$

$$S(q) = 1 + N_{\text{p}} \int 4\pi r^2 [g(r) - 1] \frac{\sin(qr)}{qr} dr \quad (7)$$

where N_{p} is the number density of particles, as defined in eq 2. The correlation function, $g(r)$, was obtained by solving the Ornstein-Zernike (OZ) equation (eq 8) by using the mean-spherical approximation (MSA) closure relation (eq 9)

$$h(r_{12}) = c(r_{12}) + \rho \int dr_3 c(r_{13}) h(r_{23}) \quad (8a)$$

$$h(r) = g(r) - 1 \quad (8b)$$

where $r = r_{ij}$ the distance between a pair of particles, $h(r)$ is total correlation function, and $c(r)$ is the direct correlation function. If $c(r)$ can be expressed by the interaction potential, $U(r)$, the OZ equation becomes a closed integral equation for $h(r)$.

In the MSA,

$$c(r) = -U(r)/k_{\text{B}} T \text{ for } r > 2R \quad (9a)$$

$$h(r) = -1 \text{ for } r < 2R \quad (9b)$$

The closed analytical form of the direct correlation function, $c(r)$, and the structure factor, $S(q)$, were obtained by Hayter and Penfold (see ref 43 for details).

Square-Well Structure Factor, $S_{\text{SW}}(q)$: At a high salt concentration, the surface charges are highly screened, and a net attractive potential is found for many protein systems.^{5,6,12,13,30} This net attractive potential may originate from van der Waals

interactions, with the depletion force caused by excluding the volume of ions or other interactions such as hydration forces or a hydrophobic force. In this work, a square-well potential is used to describe the net attractive interaction at high ionic strength, which is characterized by a hard-core repulsion for small interparticle distances, and by a constant attraction potential within a narrow shell (eq 10)⁴⁵

$$U_{\text{sw}}(r) = \begin{cases} \infty & \text{for } r < 2R \\ -\Delta & \text{for } 2R \leq r \leq 2R\delta \\ 0 & \text{for } r > 2R\delta \end{cases} \quad (10)$$

where Δ is the well depth. Positive well depths correspond to an attractive potential, and negative well depths correspond to a potential “shoulder”; δ is the well width defined as multiples of the particle diameter ($2R$). Thus, the interaction separation between a pair of particles is $2R(\delta - 1)$. An analytical form of the structure factor was obtained by Sharma et al. by solving the Ornstein–Zernike equation in the mean-spherical approximation.⁴⁵ This solution has been compared to Monte Carlo simulations for a square-well fluid, showing the limitation of the application to a well depth of $\Delta < 1.5k_{\text{B}}T$ and a volume fraction of $\phi < 0.08$.³⁷

Hard-Sphere Structure Factor, $S_{\text{HS}}(q)$: At moderate ionic strength, the surface charge is sufficiently screened. The overall interparticle interaction is rather weak, and the protein molecules interact with each other mainly through hard-sphere (excluded-volume effect) interactions.⁴⁶

$$U_{\text{HS}}(r) = \begin{cases} \infty & \text{for } r < 2R \\ 0 & \text{for } r > 2R\delta \end{cases} \quad (11)$$

In this case, the OZ equation is solved by using the Percus–Yevick (PY) closure^{37,46}

$$c(r) = g(r)[1 - \exp(U_{\text{HS}}(r)/k_{\text{B}}T)] \quad (12)$$

where $g(r)$ is the pair correlation function. Within the PY closure, the OZ equation can be solved numerically. The structure factor, $S_{\text{HS}}(q)$, was then obtained by eq 7.

4. Results and Discussion

In the remainder of this paper, the form factor is always assumed to be that of an oblate ellipsoid with radii of $a \times b \times b = 17 \times 42 \times 42 \text{ \AA}$. All of the structure factors from data fitting are effective structure factors, which are calculated using an effective sphere diameter of an ellipsoidal protein molecule.^{36,37} The results are organized according to ionic strength.

4.1. Low Ionic Strength, $I < 0.3 \text{ M}$, Data Fit by the E+SC Model. In a dilute protein solution, with added salt to screen the electrostatic interaction, the total scattering intensity is the sum of the scattering of individual molecules. The data for 10 mg/mL BSA with 0.3 M NaCl have been fitted using different form factors, such as a sphere, a prolate ellipsoid, and an oblate ellipsoid, as shown in Figure 1. The front view of the space-filling model of a serum albumin molecule is shown as an inset to Figure 1. The yellow, red, and blue parts represent the neutral, acidic, and basic residues, respectively.⁴¹ It is clear that, although the fitted data using all three of the form factors fit the experimental scattered intensity well for $q < 0.1 \text{ \AA}^{-1}$, the oblate ellipsoid form factor with $a = 17 \text{ \AA}$ and $b = 42 \text{ \AA}$ fits the data best up to 0.25 \AA^{-1} . On the basis of many data sets from dilute solutions, we found that an oblate ellipsoid form factor with $a = 17 \pm 1 \text{ \AA}$ and $b = 42 \pm 1 \text{ \AA}$ is the best description for the shape of BSA molecules in solution and gives a radius of

gyration of 27.6 \AA . These values were fixed in the following data-fitting procedure.

As pointed out by Hayter and Penfold,^{43,44} at low ionic strength, the weakly attractive van der Waals part of the colloid (DLVO) potential will have little effect on the time-averaged structure because the repulsive, screened Coulomb potential is much larger than thermal energies at small interparticle separations. The structure factor proposed by these authors has been successfully used to predict the pronounced interaction peaks in small-angle neutron scattering (SANS) experiments for micellar solutions and protein solutions.^{38,39,47} The scattering intensity was fitted using an ellipsoid form factor combined with the screened Coulomb structure factor (E+SC).

Figure 2a shows the experimental scattering intensity distribution and simulations for protein solutions with no added salt. When the protein concentration is less than 10 mg/mL, the solution is dilute, protein molecules are well-separated, and n interactions between them are observed ($\bar{S}(q) = 1$); the total scattering intensity is the sum of the scattering of the individual molecules. The experimental intensity profiles can be fitted by an oblate ellipsoid form factor.

With increasing protein concentration, a pronounced correlation peak at finite q was observed, and the peak position changed with the protein concentration; the peak shifted to higher q values, and its intensity initially increased and reached a maximum at 300 mg/mL before decreasing. Figure 2b shows the data at low ionic strength, $I = 0.05 \text{ M}$. The data can be fitted by including a form factor only, up to 20 mg/mL. The correlation peaks for higher protein concentrations ($c \geq 40 \text{ mg/mL}$) are broadened and have a higher scattering intensity at a low q range compared with those for the data with no added salt (Figure 2a). However, at such a low ionic strength, the interaction can still be described by a screened Coulombic potential. Similar results were obtained for the data fitting at $I = 0.1 \text{ M}$ (Figure 2c); the repulsive interaction is further reduced as expected.

The effective structure factors, $S_{\text{SC}}(q)$, calculated from the fitting parameters are plotted in Figure 3. Figure 3a presents the evolution of $S_{\text{SC}}(q)$ with protein concentration with no added salt. The structure factor at $q = 0$ is equal to the normalized osmotic compressibility. A screened Coulombic structure factor of $S_{\text{SC}}(0) < 1$ indicates the dominance of the repulsive interaction, while the decrease of $S_{\text{SC}}(0)$ with protein concentration suggests the increase of a repulsive force. The first peak of $S_{\text{SC}}(q)$ represents the correlation between a pair of protein molecules in the solution. The peak position shifts to higher q values, suggesting a decrease in the correlation distance with increasing protein concentration. Figure 3b presents the evolution of $S_{\text{SC}}(q)$ for BSA (100 mg/mL) with ionic strength. $S_{\text{SC}}(0)$ increases with increasing ionic strength, and the first peak becomes broad and shifts its position to a higher q value. Therefore, an increase in ionic strength decreases the repulsive force and weakens the correlation between protein molecules in solution.

The temperature, T (293 K), the dielectric constant of water ($\epsilon = 80.1$), and form factor dimensions were fixed during the fitting procedure, and the variables, ionic strength (I), surface charge (z), and volume fraction (ϕ), were used as fitting parameters. The fit parameters are summarized in Table 1. We found that the volume fraction is systematically higher than the calculated value. Chen and co-workers studied BSA solutions by small-angle neutron scattering (SANS),^{38,39} and they fitted their data by assuming a prolate ellipsoid with $a/b = 3.5$, combined with the structure factor proposed by Hayter and

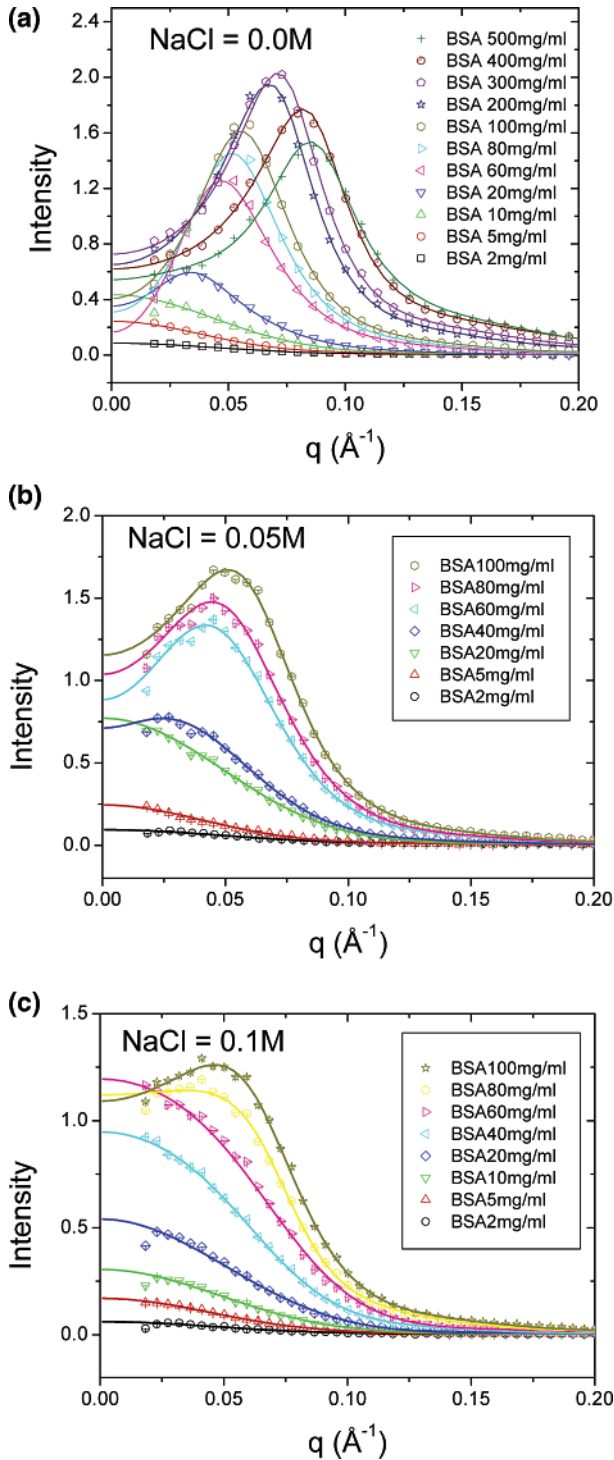


Figure 2. Scattered intensity and theoretical fit by an ellipsoidal form factor and screened Coulomb potential model (E+SC) for a wide range of protein concentrations at a lower ionic strength. (a) $I = 0.0\text{M}$, the data of very low protein concentrations (2, 5, and 10 mg/mL) were fitted using an ellipsoidal form factor only; (b) $I = 0.05\text{M}$, the data of 2, 5, and 20 mg/mL were fitted using an ellipsoidal form factor only; and (c) $I = 0.1\text{M}$, the data of BSA (2–20 mg/mL) were fitted using an ellipsoidal form factor only. Only every 10th data point is shown for clarity. The error bar is estimated to be smaller than the size of the marker.

Penfold.^{43,44} Although the fits were satisfactory, they found that the measured volume fraction is always smaller than the true values. It is interesting to note that, when the prolate ellipsoidal form factor is used to fit the data, in this work, the fitted volume fractions are smaller than the calculated value. Therefore, we

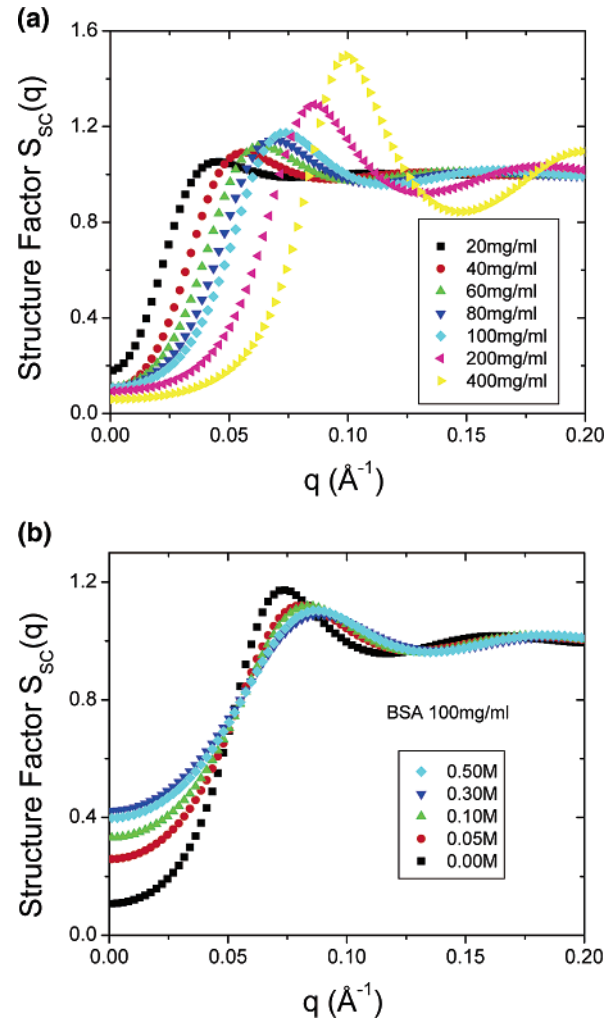


Figure 3. Structure factor, $S_{sc}(q)$ (screened Coulomb potential), calculated from Figure 2 as a function of protein concentration (a) and ionic strength (b).

TABLE 1: Fitting Parameters for an Ellipsoidal Form Factor Plus Screened Coulomb Potential Model (E+SC) for a BSA Solution with Low Ionic Strength^a

c (mg/mL)	NaCl (M)	ϕ (%)	fitted charge	ionic (10^{-3}M)	κ_D^{-1} (nm)	
20	0	1.38	1.45	10	0.91	0.96
40	0	2.97	3.76	10	1.4	0.77
60	0	4.65	5.93	11	1.5	0.75
80	0	6.13	7.98	12	3.0	0.53
100	0	7.55	10.0	13	5.8	0.37
	0.05		9.81	14	44.6	0.14
	0.1		9.42	23	161	0.072
	0.3		8.87	21	285	0.054
	0.5		9.00	36	506	0.041
200	0	14.5	16.9	18	32	0.16
300	0	19.2	20.2	17	38	0.15
400	0	23.2	29.4	9	9.8	0.29
500	0	27.4	32.8	7	3.5	0.49

^a The errors of the fitting parameters pertaining to the fitting procedure are better than 1%, but the systematical errors, including sample preparation, raw data correction, and calibration, are estimated to $<10\%$. The same condition applies to Tables 2 and 3.

believe that this discrepancy is due to the fact that neither the prolate nor the oblate ellipsoid can perfectly describe the shape of BSA in solution.

For the solutions with no added salt and $c \leq 100\text{mg/mL}$, the fitted ionic strength is less than 0.005 M, as expected. The surface charge ranges from 10 to 13. According to the proton

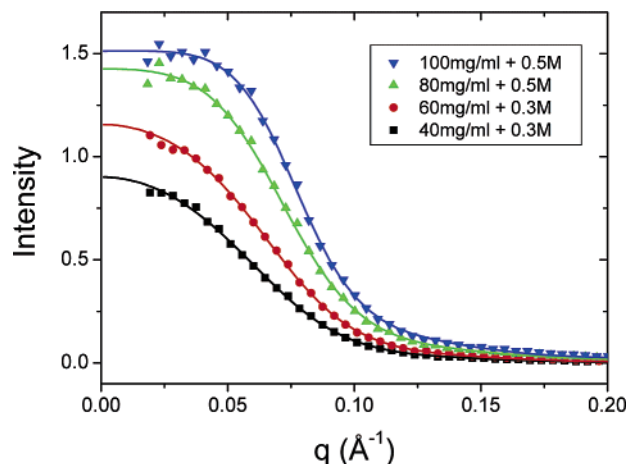


Figure 4. Scattered intensity and model fit from an ellipsoidal form factor and hard-sphere model (E+HS) at medium ionic strengths, 0.3 and 0.5 M. Only every 10th data point is shown for clarity.

TABLE 2: Fitting Parameters from an Ellipsoidal Form Factor and Hard-Sphere Model (E+HS) for Protein Solutions with Moderate Ionic Strength

c (mg/mL)	NaCl (M)	ϕ (%)	fitted ϕ (%)
40	0.3	2.97	2.94
60	0.3	4.65	5.70
80	0.5	6.13	8.37
100	0.5	7.55	10.1

titration result⁴⁸ and chloride anion binding data of Scatchard et al.,⁴⁹ the BSA molecule in a pH = 7.0 solution, and without added salt, has a negative charge value around 10; when 0.3 M LiCl is added, the charge increases to 20. The results of the fit to the present data for $c = 100$ mg/mL with increasing ionic strength are also presented in Table 1. The surface charge increased with ionic strength, as is expected due to the binding of chloride anions.⁴⁹

4.2. Moderate Ionic Strength, $I = 0.3$ and 0.5 M. With increasing ionic strength, due to screening, both the range and the strength of the interaction are decreased. At $I = 0.3$ or 0.5 M, the ionic strength is so high that almost all electrostatic interactions are screened. Although the experimental scattering intensity at protein concentrations of less than 40 mg/mL can still be satisfactorily fitted by the form factor only, it fails to fit the data with higher protein concentrations. When using a hard-sphere structure factor, the fit is reasonably good, as shown in Figure 4, and the fitted volume fraction is also higher, as summarized in Table 2. The interaction potential seems to depend strongly on the protein concentration. For example, at $c = 100$ mg/mL and $I = 0.3$ and 0.5 M, the data can also be fitted by E+SC, as shown in Table 1. The repulsive potential at a high protein concentration may be due to the binding of anions. Nossal et al.³⁹ studied the BSA in an unbuffered solution with 0.2 M NaCl, and they found that a Yukawa form of the potential could be used to fit the experimental data. However, the obtained surface charge was unrealistically high (up to 100).

4.3. High Ionic Strength, $I > 0.5$ M, Data Fit by the E+SW Model. Graphs (a) and (b) of Figure 5 show the data at a very high ionic strength, $I = 1.0$ and 2.0 M, respectively. Similar results were observed for $I = 1.5$ M (data not shown). The increase of the low q -range scattering intensity indicates the presence of an attractive potential. Figure 5c indicates that the forward intensity, $I(0)$, decreases with ionic strength. The data for low protein concentration ($c < 10$ mg/mL) were fitted by the form factor only. The attractive interaction dominated in other samples and the data can be fitted well by combining

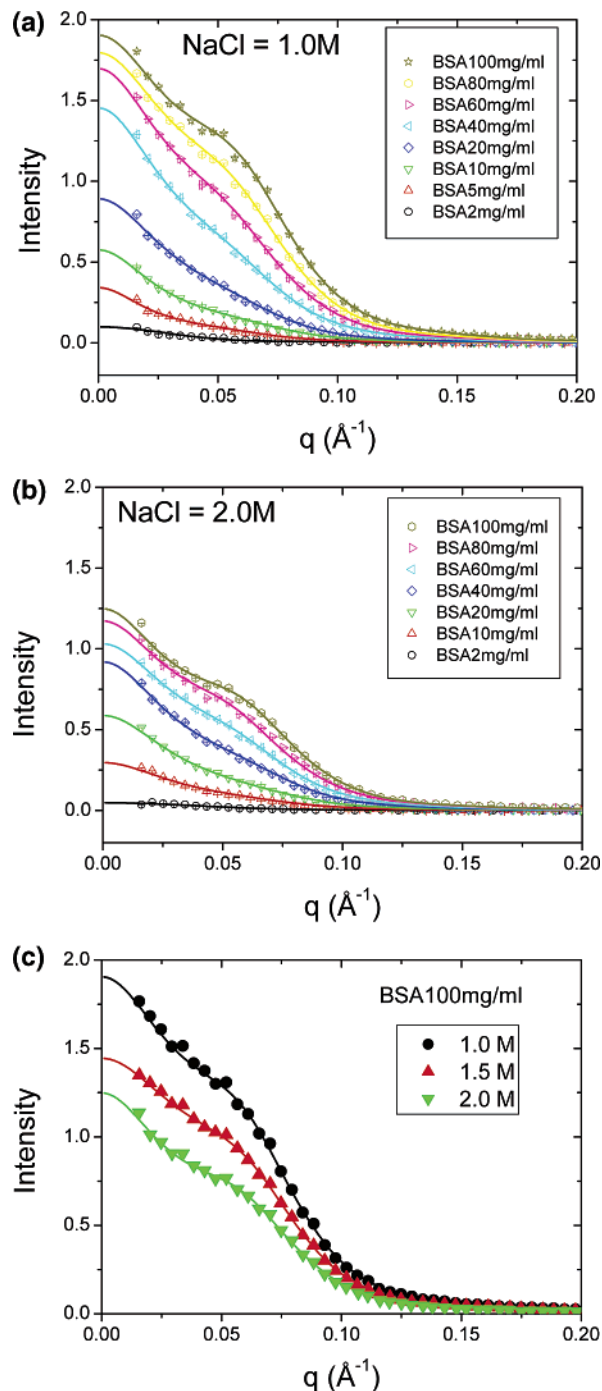


Figure 5. Scattered intensity and theoretical fit from an ellipsoidal form factor and square-well model (E+SW) for protein solutions at high ionic strength. (a) $I = 1.0$ M, the data of very low protein concentrations (2 and 5 mg/mL) were fitted using an ellipsoidal form factor only; (b) $I = 2.0$ M, the data of 2 mg/mL were fitted using an ellipsoidal form factor only; and (c) $c = 100$ mg/mL with different ionic strengths. Note that the data of the very low protein concentration were fitted using an ellipsoidal form factor only (see text). Only every 10th data point is shown for clarity.

the form factor with a square-well structure factor. The fit parameters are given in Table 3. In all of the fits, positive well depth values were obtained, which indicated the presence of an attractive interaction. The strength of the attraction decreased with increasing protein concentration, from 1.5 to $0.04k_B T$. At the same time, the well width increased with protein concentration from 1.6 to 2.5, implying that the interaction is a medium-to long-range interaction.

TABLE 3: Fitting Parameters from an Ellipsoidal Form Factor and Square-Well Potential Model (E+SW) for Protein Solutions with a High Ionic Strength, $I \geq 1.0$ M

c (mg/mL)	NaCl (M)	ϕ (%)	well depth ($k_B T$)	well width δ
10	1.0	0.708	1.24	1.83
	1.5		1.5	1.65
	2.0		1.5	1.66
20	1.0	1.51	0.462	1.85
	1.5		0.691	1.57
	2.0		0.996	1.59
40	1.0	2.97	0.199	1.94
	1.5		0.259	1.80
	2.0		0.305	1.82
60	1.0	4.65	0.079	2.20
	1.5		0.135	2.06
	2.0		0.105	2.05
80	1.0	6.13	0.047	2.45
	1.5		0.052	2.34
	2.0		0.065	2.21
100	1.0	7.55	0.041	2.43
	1.5		0.040	2.34
	2.0		0.070	2.22

Figure 6 shows the effective structure factor, $S_{SW}(q)$, calculated from the fitting parameters. The evolution of $S_{SW}(q)$ as a function of protein concentration (Figure 6a) and ionic strength (Figure 6b) is quite different than that of $S_{SC}(q)$ (Figure 3). With increasing protein concentration, $S_{SW}(0)$ decreases. Once the attractive potential dominates, an increase in the ionic strength only slightly affects $S_{SW}(q)$ (i.e., $S_{SW}(0)$ increases only slowly with I). It is worth noting that the square-well model contains both a repulsive (hard-sphere potential) and an attractive part in the potential (eq 10). The contribution to the total structure factor from the hard-sphere potential is presented in Figure 6c, which shows a strong volume dependence in the low q range. Therefore, the decrease of $S_{SW}(0)$ with increasing protein concentration is mainly due to the excluded-volume effect.

Other potential models, such as a sticky hard-sphere model with the PY closure, have also been tested (data not shown). The sticky hard-sphere (SHS) structure describes a narrow, attractive square-well potential.^{50,51} The mathematics behind the SHS structure factor (the PY closure) is much more appropriate for an attractive potential. However, the fitting parameters were unrealistic. Therefore, there may be additional effects such as the formation of a small amount of aggregation or clustering or other interactions involved, as discussed below. In this case, a more complex potential may be needed, such as the two-Yukawa potential model used by Liu et al., in order to simulate a mixed potential.⁵² However, these refinements are beyond the scope of this paper, the goal of which is to obtain an interaction phase diagram, such as Figure 7.

According to Kuehner et al.,¹⁵ the attractive interaction at a high salt concentration, caused by the excluded-volume effect of ions, gives rise to a strong (several $k_B T$), short-range (a few Å) attractive potential. However, in our results, although the attractive interaction dominates the overall interaction potential between proteins, we find that this potential is a rather weak ($< 1k_B T$), long-range potential, extending up to several tens of Å, that can be satisfactorily described by a square-well structure factor (Table 3). On the other hand, an overall attractive interaction potential will lead to aggregation or gelation. Yet, for all of the solutions investigated in this work, no matter how high the ionic strength, no aggregation or gelation was observed visually. Thus, we believe that there must be a short-range, repulsive potential dominating when proteins are very close to each other. The hydration force may be the most likely source of a short-range, repulsive potential.²⁹ Arakawa and Timasheff⁵³ studied the preferential interactions of BSA in a concentrated

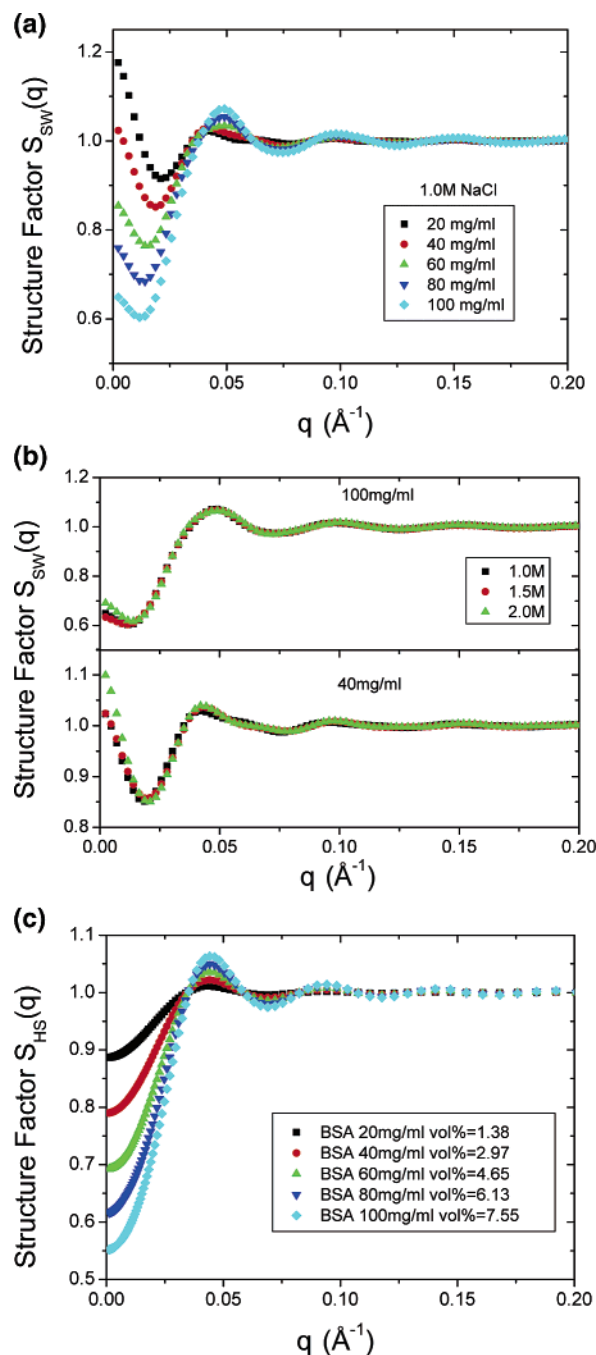


Figure 6. Calculated structure factor, $S_{SW}(q)$, as a function of protein concentration (a) and ionic strength (b). Graph c presents the contribution of the hard-sphere effect to the overall structure factor, $S_{SW}(q)$, as a function of protein concentration.

salt solution, and they found that proteins are preferentially hydrated at a high concentration of NaCl.

Our results presented above indicate that, in order to fully understand the protein–protein interaction in solution, the interaction between a protein and salt has to be taken into account. It has been shown that up to a moderate salt concentration ($I \sim 0.1$ – 0.3 M), the neutralization of charges on the protein is dominant, which leads to a “salting in” effect. This is in good agreement with our observations that chloride anions prefer to bind on the surface of a protein and increase the surface charges, as shown in Table 1. At a high salt concentration, the protein–salt interaction is dominated by the unfavorable interaction between the salt ions and the hydrophobic residues of the protein, producing a “salting out” effect.

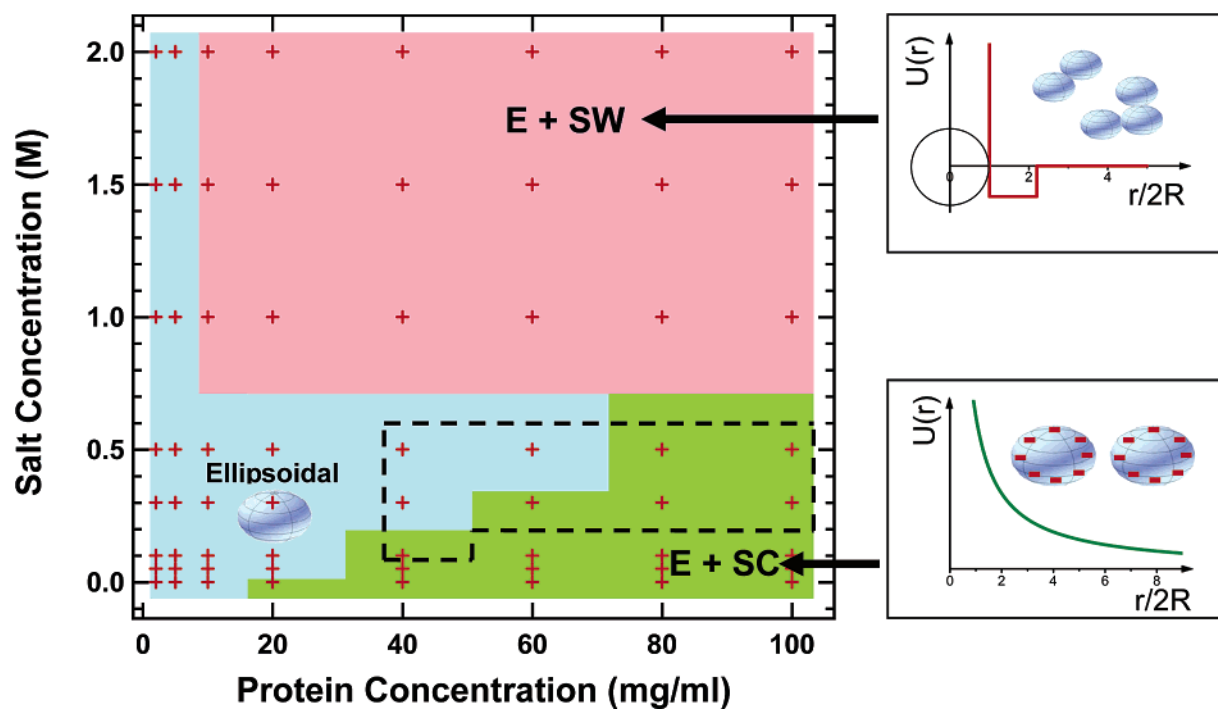


Figure 7. Approximate phase diagram of the interaction as a function of protein concentration and ionic strength, based on the model described in section 3. Note that the boundaries are, of course, not thought to be sharp. In the map, “Ellipsoidal” means the data were fitted by a form factor only. E+SC: data fitting by an ellipsoidal form factor combined with a screened Coulombic structure factor. E+SW: ellipsoidal form factor combined with square-well structure factor.

Depending on the hydration property of the ions, a kosmotrope (strongly hydrated ion) can stabilize proteins at a high concentration, but chaotropes (weakly hydrated ion) at high concentrations destabilize proteins due to the direct interactions with the protein.^{14,54} Sodium chloride is a kosmotrope,⁵⁴ which tends to stabilize the protein at a high salt concentration. Combined with the hydration effect, which results in a short-range, repulsive interaction between a pair of proteins, it is reasonable that the overall weak and long-ranged attraction does not lead to the aggregation of proteins.

4.4. Interaction Phase Diagram. An interaction phase diagram showing the complete set of data over a wide range of protein concentrations and ionic strengths is given in Figure 7. Following from our fitting results, the solution phase behavior can be divided into three regions based on the protein–protein interaction. At a low protein concentration, combined with the screening effect of adding salt, the solutions are approaching ideal behavior, that is, there are no correlations between protein molecules. The scattering intensity can be successfully fitted using an oblate ellipsoid form factor. With increasing protein concentration, while keeping the ionic strength low, the screened Coulomb repulsive interaction dominates the overall interaction between protein molecules. The intensity spectra can be fitted satisfactorily by taking into account both the form factor and an interference structure factor, $\bar{S}(q)$. The calculation of $\bar{S}(q)$ is based on the interaction potential between charged colloidal particles consisting of a hard sphere plus a screened Coulomb potential. At very high salt concentrations, $I \geq 1.0$ M, the interaction potential between protein molecules is dominated by an attractive potential. The data can be fitted using a form factor plus a square-well structure factor. However, in contrast to the strong, short-range potential predicted from the depletion effect under a high salt concentration, our results show a weak and long-range, attractive potential, which strongly depends on the protein concentration.

It should be noted that the boundaries between the three regions are, of course, not sharp and that the data are not directly inverted, but rather they are fitted using model potentials. While this procedure gives reasonably realistic results, it certainly also has its limit. For example, in the area enclosed by the dashed polygon (Figure 7), the overall interaction is rather weak. In this region, none of the mentioned form and structure factors lead to satisfactory fits. It is likely that a more sophisticated structure factor is necessary to describe the interaction behavior in this salt and protein concentration range by considering the detailed anion binding, hydration, etc.

5. Conclusions

From the results obtained by fitting the data and analysis of the calculated, effective structure factor, it can be seen that, with the addition of salt (increasing the ionic strength), the protein interaction potential changes smoothly from a repulsive to an attractive potential. Without salt addition or at a low ionic strength ($I < 0.3$ M), the screened Coulomb structure factor is sufficient to describe the repulsion-dominated interaction potential. At a moderate ionic strength ($I \sim 0.3$ – 0.5 M), the surface charges are completely screened, and the interaction can be described by a hard-sphere potential with a high volume fraction. At a high ionic strength, $I \geq 1.0$ M, the overall protein–protein interaction is dominated by an attractive potential. Whereas theory predicts that the depletion force induced by a high salt concentration is a strong, short-range attractive potential, it appears that it can also be a rather weak, long-range, attractive potential. The stability of a concentrated protein solution under high salt concentration is explained by the hydration effect, which results in a short-range, repulsive force. Repulsive interaction, screened Coulomb structure factors, $S_{SC}(q)$, calculated from the fitting parameters, show a strong dependence on both protein concentration and ionic strength. The repulsion force increases with protein concentration and

decreases with ionic strength. The evolution of square-well structure factors, $S_{sw}(q)$, indicates that the attractive force decreases with protein concentration, and it only slightly increases with ionic strength for $I > 1.0$ M.

Acknowledgment. We gratefully acknowledge financial support from EPSRC and the CCLRC for the allocation of beamtime on beamline 6.2 at the SRS. We are indebted to Professor J. Penfold for his critical comments on the manuscript. We are also indebted to Steve Kline and Yun Liu at NIST for their valuable suggestions on data fitting.

References and Notes

- (1) Durbin, S. D.; Feher, G. *Annu. Rev. Phys. Chem.* **1996**, *47*, 171.
- (2) Anderson, V. J.; Lekkerkerker, H. N. W. *Nature* **2002**, *416*, 811.
- (3) Piazza, R. *Curr. Opin. Colloid Interface Sci.* **2004**, *8*, 515.
- (4) George, A.; Wilson, W. *Acta Crystallogr., Sect. D* **1994**, *50*, 361.
- (5) Tardieu, A.; Le Verge, A.; Malfois, M.; Bonneté, F.; Finet, S.; Riès-Kautt, M.; Belloni, L. *J. Cryst. Growth* **1999**, *196*, 193.
- (6) Bonneté, F.; Finet, S.; Tardieu, A. *J. Cryst. Growth* **1999**, *196*, 403.
- (7) Bonneté, F.; Vivarès, D. *Acta Crystallogr., Sect. D* **2002**, *58*, 1571.
- (8) Muschol, M.; Rosenberger, F. *J. Chem. Phys.* **1995**, *103*, 10424.
- (9) Muschol, M.; Rosenberger, F. *J. Chem. Phys.* **1997**, *107*, 1953.
- (10) Kulkarni, A. M.; Dixit, N. M.; Zukoski, C. F. *Faraday Discuss.* **2003**, *123*, 37.
- (11) Delaye, M.; Tardieu, A. *Nature* **1983**, *302*, 415.
- (12) Lonetti, B.; Fratini, E.; Chen, S. H.; Baglioni, P. *Phys. Chem. Chem. Phys.* **2004**, *6*, 1388.
- (13) Baglioni, P.; Fratini, E.; Lonetti, B.; Chen, S. H. *J. Phys.: Condens. Matter* **2004**, *16*, S5003.
- (14) Curtis, R. A.; Prausnitz, J. M.; Blanch, H. W. *Biotechnol. Bioeng.* **1998**, *57*, 11.
- (15) Kuehner, D. E.; Blanch, H. W.; Prausnitz, J. M. *Fluid Phase Equilib.* **1996**, *116*, 140.
- (16) Israelachvili, J. *Intermolecular and surface forces*; Academic Press: New York, 1992.
- (17) Pellicane, G.; Costa, D.; Caccamo, C. *J. Phys.: Condens. Matter* **2004**, *16*, S4923.
- (18) Broide, M. L.; Tominc, T. M.; Saxowsky, M. D. *Phys. Rev. E: Stat. Phys., Plasmas, Fluids, Relat. Interdiscip. Top.* **1996**, *53*, 6325.
- (19) Narayanan, J.; Liu, X. Y.; *Biophys. J.* **2003**, *84*, 523.
- (20) Velev, O. D.; Kaler, E. W.; Lenhoff, A. M. *Biophys. J.* **1998**, *75*, 2682.
- (21) Striolo, A.; Bratko, D.; Wu, J. Z.; Elvassore, N.; Blanch, H. W.; Prausnitz, J. M. *J. Chem. Phys.* **2002**, *116*, 7733.
- (22) Taratuta, V. G.; Holschbach, A.; Thurston, G. M.; Blankschtein, D.; Benedek, G. B. *J. Phys. Chem.* **1990**, *94*, 2140.
- (23) Thomson, J. A.; Schurtenberger, P.; Thurston, G. M.; Benedek, G. B. *Proc. Natl. Acad. Sci. U.S.A.* **1987**, *84*, 7079.
- (24) Foffi, G.; McCullagh, G. D.; Lawlor, A.; Zaccarelli, E.; Dawson, K. A.; Sciortino, F.; Tartaglia, P.; Pini, D.; Stell, G. *Phys. Rev. E: Stat. Phys., Plasmas, Fluids, Relat. Interdiscip. Top.* **2002**, *65*, 031407.
- (25) Stradner, A.; Sedgwich, H.; Cardinaux, F.; Poon, W. C. K.; Egelhaaf, S. U.; Schurtenberger, P. *Nature* **2004**, *432*, 492.
- (26) Stradner, A.; Thurston, G. M.; Schurtenberger, P. *J. Phys.: Condens. Matter* **2005**, *17*, S2805.
- (27) Malfois, M.; Bonneté, F.; Belloni, L.; Tardieu, A. *J. Chem. Phys.* **1996**, *105*, 3290.
- (28) Sciortino, F.; Mossa, S.; Zaccarelli, E.; Tartaglia, P. *Phys. Rev. Lett.* **2004**, *93*, 055701.
- (29) Petsev, D. N.; Vekilov, P. G. *Phys. Rev. Lett.* **2000**, *84*, 1339.
- (30) Liu, Y.; Fratini, E.; Baglioni, P.; Chen, W. R.; Chen, S. H. *Phys. Rev. Lett.* **2005**, *95*, 118102.
- (31) Stradner, A.; Cardinaux, F.; Schurtenberger, P. *Phys. Rev. Lett.* **2006**, *96*, 219801.
- (32) Kozak, M. *J. Appl. Crystallogr.* **2005**, *38*, 555.
- (33) Cernik, R. J.; Barnes, P.; Bushnell-Wye, G.; Dent, A. J.; Diakun, G. P.; Flaherty, J. V.; Greaves, G. N.; Heeley, E. L.; Helsby, W.; Jacques, S. D. M.; Kay, J.; Rayment, T.; Ryan, A.; Tang, C. C.; Terrill, N. J. *J. Synchrotron Radiat.* **2004**, *11*, 163.
- (34) Orthaber, D.; Bergmann, A.; Glatter, O. *J. Appl. Crystallogr.* **2000**, *33*, 218.
- (35) Hayter, J. B.; Penfold, J. *Colloid Polym. Sci.* **1983**, *261*, 1022.
- (36) Isihara, A. *J. Chem. Phys.* **1950**, *18*, 1446.
- (37) SANS Manuals and Data Reduction. <http://www.ncnr.nist.gov/programs/sans/data/index.html>.
- (38) Bendedouch, D.; Chen, S. H. *J. Phys. Chem.* **1983**, *87*, 1473.
- (39) Nossal, R.; Glinka, C. J.; Chen, S. H. *Biopolymers* **1986**, *25*, 1157.
- (40) Carter, D. C.; He, X. M.; Munson, S. H.; Twigg, P. D.; Gernet, K. M.; Broom, M. B.; Miller, T. Y. *Science* **1989**, *244*, 1195.
- (41) Carter, D. C.; Ho, J. X. *Adv. Protein Chem.* **1994**, *45*, 153.
- (42) Ferrer, M. L.; Duchowicz, R.; Carrasco, B.; de la Torre, J. G.; Acuña, A. U. *Biophys. J.* **2001**, *80*, 2422.
- (43) Hayter, J. B.; Penfold, J. *Mol. Phys.* **1981**, *42*, 109.
- (44) Hansen, J. P.; Hayter, J. B. *Mol. Phys.* **1982**, *46*, 651.
- (45) Sharma, R. V.; Sharma, K. C. *Physica A* **1977**, *89*, 213.
- (46) Ashcroft, N. W.; Lekner, J. *Phys. Rev.* **1966**, *145*, 83.
- (47) Bendedouch, D.; Chen, S. H. *J. Phys. Chem.* **1984**, *88*, 648.
- (48) Tanford, C.; Swanson, S. A.; Shore, W. S. *J. Am. Chem. Soc.* **1955**, *77*, 6414.
- (49) Scatchard, G.; Scheinberg, I. H.; Armstrong, S. H. Jr. *J. Am. Chem. Soc.* **1950**, *72*, 535.
- (50) Baxter, R. J. *J. Chem. Phys.* **1968**, *49*, 2770.
- (51) Menon, S. V. G.; Manohar, C.; Srinivasa Rao, K. *J. Chem. Phys.* **1991**, *95*, 9186.
- (52) Liu, Y.; Chen, W. R.; Chen, S. H. *J. Chem. Phys.* **2005**, *122*, 044507.
- (53) Arakawa, T.; Timasheff, N. *Biochemistry* **1982**, *21*, 6545.
- (54) Collins, K. D. *Biophys. J.* **1997**, *72*, 65.